Selenocysteine versus Cysteine Reactivity: A Theoretical Study of Their Oxidation by Hydrogen Peroxide

Bruno Cardey and Mironel Enescu*

University of Franche-Comte, Laboratoire de Microanalyses Nucleaires, UMR CEA E4, 16 route de Gray, 25030 Besancon, France

Received: September 7, 2006; In Final Form: November 14, 2006

The cysteine and selenocysteine oxidation by H_2O_2 in vacuo and in aqueous solution was studied using the integrated molecular orbital + molecular orbital (IMOMO) method combining the quadratic configuration method QCISD(T) and the spin projection of second-order perturbation theory PMP2. It is shown that including in the model system of cysteine (selenocysteine) residue up to 20 atoms has significant consequences upon the calculated reaction energy barrier. On the other hand, it is demonstrated that free cysteine and selenocysteine have very similar reaction energy barriers, 77−79 kJ mol^{-1} in aqueous solution. It is thus concluded that the high experimental reaction rate constant reported for the oxidation of the selenocysteine residue in the glutathione peroxidase (GPx) active center is due to an important interaction between selenocysteine and its molecular environment. The sensitivity of the calculated energy barrier to the dielectric constant of the molecular environment observed for both cysteine and selenocysteine as well as the catalytic effect of the NH group emphasized in the case of cysteine supports this hypothesis.

Introduction

Among the reactive oxygen species (ROS) present in the living cell, hydrogen peroxide (H_2O_2) has a rather weak reactivity. Its importance comes from the fact that it is a byproduct of the normal aerobic cell metabolism,[1] hence, its concentration in the biological environment is significant. H_2O_2 is reduced in an oxidoreduction cycle involving principally the glutathione peroxidase enzyme (GPx).[2] In a first step, hydrogen peroxide is reduced into water by a selenocysteine residue in the active center of the enzyme:

$$\text{GPx-Se}^- + \text{H}_2\text{O}_2 \rightarrow \text{GPx-SeO}^- + \text{H}_2\text{O} \qquad (1)$$

Then, the oxidized enzyme is regenerated in reaction with the glutathione (GSH):

$$\text{GPx-SeO}^- + 2\text{GSH} \rightarrow \text{GPX-Se}^- + \text{GSSG} + \text{H}_2\text{O} \qquad (2)$$

The rate constant of the H_2O_2 reduction reaction is significantly enhanced because at physiological pH the selenocysteine is deprotonated. Indeed, the selenol/selenolate pK_a of free selenocysteine is only 5.2,[3] significantly smaller than 8.4 that is the thiol/thiolate pK_a of free cysteine.[4] On the other hand, the cysteine, even deprotonated, reduces the H_2O_2 at a rate constant of only 16−21 mol^{-1} dm^3 s^{-1} (refs 5, 6) which is considerably smaller than the rate constant reported for the corresponding GPx reaction (5.0×10^7 mol^{-1} dm^3 s^{-1}).[7,8] To explain this enormous difference between two systems which do not seem fundamentally different, we have recently analyzed at theoretical level the H_2O_2 reduction by two model systems, methanethiolate and methaneselenolate.[9] The calculations predicted similar reactivities for the two systems and it was concluded that the selenolate environment in the enzyme does play an important role in the very high reactivity of the GPx. A natural extension of this theoretical analysis is to include into the model system all the atoms of the peptidic fragment representing the selenocysteine residue. This approach could provide information about structural factors and specific interactions affecting the reaction energy barrier. Increasing the size of the molecular system should be done without affecting in a significant manner the accuracy of the ab initio calculations. From this point of view, the integrated molecular orbital + molecular orbital (IMOMO)[10] was very promising. This method combines calculations at two different theory levels: a higher one applied to a restraint part of the quantum system and a lower one applied to the whole system. It is thus possible to preserve accuracy in treating the chemically significant part of the system and to take into account environmental effects treated at a lower level of theory. Recently, this method was successfully applied to the study of the cysteine oxidation by the hydroxyl radical.[11]

In the present paper, the reduction of hydrogen peroxide by selenolate is analyzed by including 20 atoms in the model system of the selenocysteine residue. The energy barrier of the reaction is calculated with the IMOMO method combining the QCISD(T)[12] and the MP2[13] levels of theory. The predicted selenocysteine reactivity is compared to that of cysteine and the biological significance of the results is discussed.

Computational Method

The cysteine and selenocysteine model systems were constructed starting from the amino acid structures by replacing the terminal $-NH_3^+$ and $-COO^-$ groups by the $-NH-CH_3$ and $-CO-NH-CH_3$ groups, respectively.

All calculations were carried out using GAUSSIAN 03 (ref 14) program on a Windows XP operating PC equipped with an Intel Pentium IV CPU 2.4 GHz processor and 2 GB of RAM.

The geometry optimizations were performed at the MP2/6-311+G(d,p) level of theory both in vacuo and in water. The

* To whom correspondence should be addressed. Tel.: (+33) 3 81 66 65 21. Fax: (+33) 3 81 66 65 22. E-mail: mironel.enescu@univ-fcomte.fr.

10.1021/jp0658445 CCC: $37.00
Published on Web 01/05/2007

solvent effects were taken into account by using polarizable continuum model (PCM), IEF-PCM version,[15] as it is implemented in GAUSSIAN 03. The nature of the stationary points was checked by performing frequency calculations.

The standard gas-phase Gibbs free energy (G_g) of a molecular state M was calculated as follows:

$$G_g(M) = E_{p,g}(M) + \Delta G_{c,g}(M) \quad (3)$$

Here, $E_{p,g}(M)$ is the gas-phase molar potential energy and $\Delta G_{c,g}(M)$ is the molar Gibbs free energy correction calculated at 298 K and 1 atm. The zero-point corrected energy ($E_{0,g}$) or the standard enthalpy (H_g) was obtained in a similar manner by adding to the molar potential energy the zero-point energy correction or the enthalpy correction, respectively. All these corrections are automatically given by GAUSSIAN in frequency calculation jobs. Single-point energy calculation with the IMOMO method gave the $E_{p,g}(M)$. The high-level system included the H_2O_2 and the $CH_3-S(e)^-$ fragments and was treated with the QCISD(T) method using the 6-311+G(2df,pd) basis set on sulfur (or selenium) and H_2O_2 atoms and the 6-311+G(d,p) basis set on the CH_3 atoms. The low-level system was treated at the PMP2[16]/6-311+G(d,p) level of theory. In the present case, the PMP2 method was chosen instead of the simpler MP2 method because the wave function of the transition state presented an instability with respect to the restricted Hartree−Fock→unrestricted Hatree−Fock transition. The effect of this instability on the energy calculated at the MP2 level of theory cannot be disregarded, but it is less important at a higher level of theory such as the QCISD(T) level.[9]

The standard Gibbs free energy in aqueous solution (G_{aq}) was calculated with the formula

$$G_{aq}(M) = G_g(M) + G_{solv}(M) \quad (4)$$

where G_{solv} is the PCM solvation free energy. To calculate the solvation free energy, all structures were reoptimized in the solvent at MP2/6-311+G(d,p) level of theory. Then, single-point energy calculations were performed using a larger basis set, 6-311+G(2df,2pd), at the PMP2 level of theory.

Results and Discussion

Cysteine Residue Oxidation. In a detailed experimental study, Luo et al.[17] have clearly shown that the cysteine (CSH) oxidation by H_2O_2 to cystine (CSSC) follows the sequence

$$CSH \leftrightarrow CS^- + H^+ \quad (5)$$

$$CS^- + H_2O_2 \xrightarrow{k_1} CSOH + HO^- \quad (6)$$

$$CSOH + CS^- \xrightarrow{k_2} CSSC + HO^- \quad (7)$$

In this sequence, the formation of the sulfenic acid (CSOH) is the rate-determining step. The mechanism of this step has been theoretically demonstrated[9] for the model systems methanethiolate and methaneselenolate: it consists of a simultaneous oxygen atom addition to sulfur (selenium) and a hydrogen atom transfer to the second oxygen atom of the peroxide giving $CH_3S(e)O^-$ and H_2O as products. The reaction pathway derived by intrinsic reaction coordinate (IRC)[18] calculations connects the transition state (TS) to a reactant complex (RC), to one side, and to a product complex (PC), to the other side. The RC and PC are formed by hydrogen bonding between $CH_3S(e)^-$ and H_2O_2 and, respectively, between $CH_3S(e)O^-$ and H_2O. This reaction mechanism presents similarities with that recently proposed by Chu and Trout[19] for the oxidation of dimethyl sulfide by H_2O_2, except for the catalytic role of hydrogen bonding to solvent demonstrated in this later case.

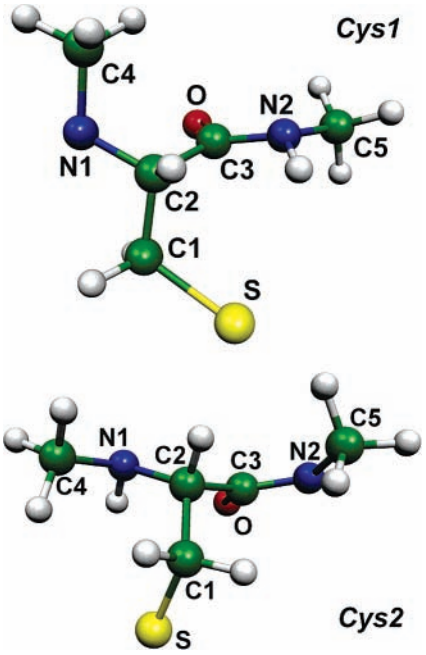

Figure 1. The cysteine residue models cys1 and cys2. Geometries were optimized in aqueous solution at the MP2/6-311+G(d,p) level of theory using the PCM solvation model.

In the present study, cysteine residue oxidation by H_2O_2 was considered either as reference for selenocysteine oxidation or as a test for the computational method. The geometry optimization of the cysteine residue model in aqueous solution gave three stationary conformations. The more stable one, cys1, is presented in Figure 1. The two other conformations are interesting too because in the protein environment their relative stabilities with respect to cys1 may change. This is the reason why we also performed energy-barrier calculations for the oxidation of a second cysteine structure, here denoted by cys2 (Figure 1). The main difference between cys1 and cys2 concerns the value of the torsion angle τ(SC1C2C3) which is 60.89° for cys1 and −68.23° for cys2.

The starting TS and RC geometries for cysteine (selenocystene) oxidation were generated by reproducing the related configurations of the H_2O_2 and S(e) atoms found for the similar reaction of the model system methanethiolate (methaneselenolate).[9] For cysteine residue cys1 we obtained, after reoptimization, the RC1 and TS1a structures given in Figure 2. The inclusion of more atoms in the reactant system affects only slightly the in vacuo geometry of the transition state: the S−O distance increases by about 0.01 Å while the S−H distance decreases by 0.03 Å with respect to the values reported for the methanethiolate model system. However, the Gibbs free energy difference ΔG_g(TS1a) between TS1a and free reactants (FR1) is now 27.0 kJ (Table 1), that is, 14.2 kJ mol^{-1} higher than in the methanethiolate case. In aqueous solution, the Gibbs free energy difference between the two states becomes 79.6 kJ mol^{-1} (Table 1) indicating that the solvent considerably destabilizes the transition state. This difference here denoted ΔG_{aq}(TS1a) is greater by about 10.6 kJ mol^{-1} with respect to that calculated for methanethiolate. Because the dissociation Gibbs free energy of the complex RC1 is only −2.0 kJ mol^{-1} (ΔG_{aq}(RC1) in Table 1), this complex plays no role in the reaction kinetics, which

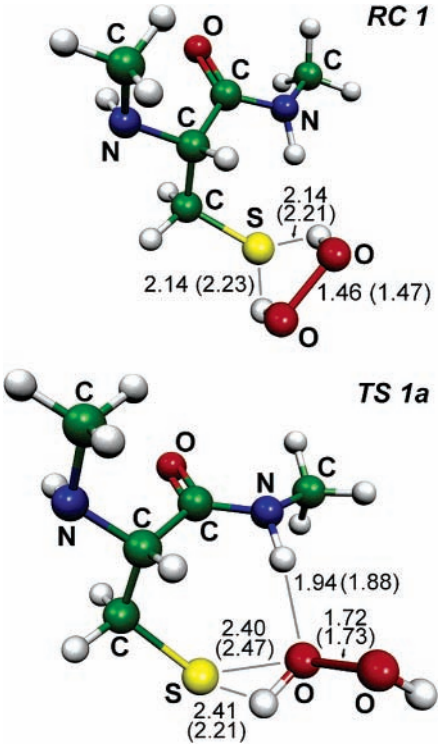

Figure 2. Oxidation of the cysteine residue model cys1 by H_2O_2: the reactant complex RC1 and the transition-state TS1a. Atomic distances are given in Å. Geometries were optimized in vacuo and in aqueous solution at the MP2/6-311+G(d,p) level of theory. The in vacuo atomic distances are given in parentheses.

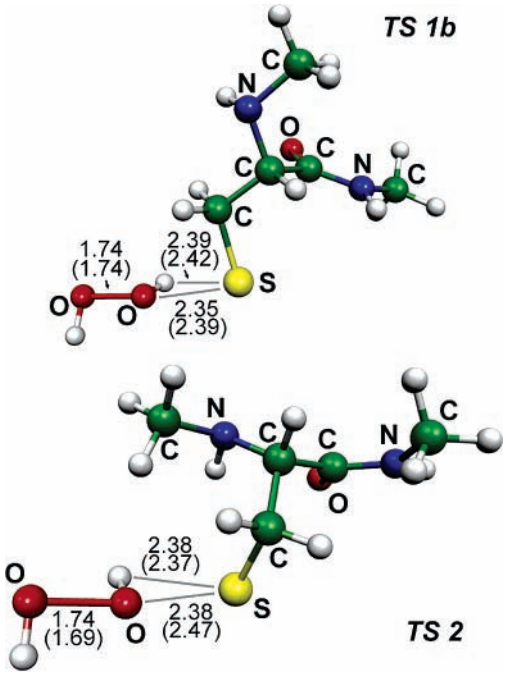

Figure 3. Transition state for the oxidation of the cysteine residue model cys2 by H_2O_2 (TS2) and an alternative transition state for the oxidation of the cysteine model cys1 (TS1b). Atomic distances are given in Å. Geometries were optimized in vacuo and in aqueous solution at the MP2/6-311+G(d,p) level of theory. The in vacuo atomic distances are given in parentheses.

will depend only on ΔG_{aq}(TS1a).[11] Hence, ΔG_{aq}(TS1a) is the effective reaction energy barrier.

The TS1a structure in Figure 2 suggests that the oxidation energy barrier for cysteine residue is affected by the H bond formed between the peroxide and the NH group of cys1. To test this hypothesis, we explored the configuration space of the two interacting fragments and found a second transition state (TS1b) for which no H bond between peroxide and NH group was present (Figure 3).

For this second reaction pathway, the energy barrier was higher: 49.4 kJ mol^{-1} in vacuo and 85.6 kJ mol^{-1} in aqueous solution. This result suggests that the H-bonding here analyzed has a catalytical effect on the cysteine oxidation. The effect is very marked in vacuo but is significantly attenuated in aqueous solution.

The statement concerning the role of the NH group in lowering the reaction energy barrier is apparently contradicted by the result obtained on the cys2 conformation. In this case also, there is no H bond between the NH group and the H_2O_2 (Figure 3), but the reaction energy barrier is only slightly higher than ΔG_g(TS1a). However, the direct comparison between cys1 and cys2 might not be very relevant because the difference between the two systems is complex. For instance, the complex RC2 formed between H_2O_2 and cys2 has a complexation Gibbs free energy ΔG_g(RC2) lower by about 14 kJ mol^{-1} with respect to ΔG_g(RC1). This result indicates a stronger attraction between the two reactants in the case of cys2 which could also displace the energy level of the transition state.

The energy values in Table 1 are not corrected for the basis set superposition errors (BSSE). These errors are due to basis set truncation and have a lowering effect on the calculated interaction energy between the two molecular fragments. On the other hand, the basis set truncation induces also an opposite effect: a rising of the interaction energy because of an approximate description of the reciprocal perturbation of the interacting subsystems.[20] Hence, BSSE correction would be useful only in case of negligible perturbations. Otherwise, the BSSE uncorrected interaction energies are expected to be closer to the experimental values because of the partial compensation of the two basis set truncation effects.[21] Obviously, a transition state is associated with a significant electronic rearrangement around the interacting atoms. Hence, in our opinion, it falls in

TABLE 1: Thermodynamic Parameters of the Free Reactants (FR), Reactant Complexes (RC), and Transition States (TS) Involved in the Cysteine Oxidation by H_2O_2[a]

	$E_{p,g}$ (Hartree)	$\Delta E_{0,g}$ (kJ mol^{-1})	ΔH_g (kJ mol^{-1})	ΔG_g (kJ mol^{-1})	G_{solv} (kJ mol^{-1})	ΔG_{aq} (kJ mol^{-1})
FR1	−930.06126	0.0	0.0	0.0	−232.2	0.0
RC1	−930.09505	−82.4	−83.3	−42.9	−187.3	2.0
TS1a	−930.06556	−13.9	−16.1	27.0	−179.6	79.6
TS1b	−930.05700	8.5	6.4	49.4	−196.0	85.6
FR2	−930.03612	0.0	0.0	0.0	−276.7	0.0
RC2	−930.07521	−96.4	−97.3	−56.8	−221.6	−1.7
TS2	−930.03972	−12.1	−14.2	28.8	−225.2	80.3

[a] IMOMO gas-phase potential energy ($E_{p,g}$), relative gas-phase zero-point-corrected energy ($\Delta E_{0,g}$), enthalpy (ΔH_g), Gibbs free energy (ΔG_g), solvation free energy (G_{solv}), and relative Gibbs free energy in aqueous solution (ΔG_{aq}). The reference states for the relative parameters are FR1 for the Cys1 model and FR2 for the Cys2 model.

that category of structures for which BSSE correction does not improve the agreement with the experimental data. The situation may be different for the RC1 state since the hydrogen bonding involves only a small rearrangement of the electronic density. In this case, the BSSE correction calculated with the counterpoise method of Boys and Bernardi[22] at the IMOMO (QCISD-(T)/PMP2) level of theory was about 8.0 kJ mol^{-1}. The BSSE corrected value of ΔG_{aq}(RC1) is thus 10.0 kJ mol^{-1}.

The thermal contributions to the Gibbs free energy values in Table 1 were calculated assuming the harmonic oscillator approximation for all the normal modes. It is known that this approximation could induce nonnegligible errors because of the presence of hindered internal rotations.[23] The corresponding corrections were evaluated for the TS1a and FR1 structures as described in ref 11 giving rise to a final alteration of ΔG_{aq}(TS1a) by about +1.5 kJ mol^{-1}.

The ab initio energy barrier we report here for the oxidation of the residue model cys1 is about 13.0 kJ mol^{-1} higher than the experimental value reported for the cysteine amino acid in aqueous solution.[17] This deviation could be partially due to the structural difference between the cysteine amino acid and cysteine residue model. Thus, it may be considered as a superior limit of the specific error of our computational method. Obviously, a significant contribution to the overall error comes from the solvation free-energy calculation. For instance, when the isodensity polarizable continuum model (IPCM)[24] is used, the calculated reaction energy barrier becomes 62.8 kJ mol^{-1}, that is, about 4 kJ mol^{-1} lower than the experimental energy barrier for the cysteine anino acide. However, we think the PCM solvation free energy is more reliable in the present case since this method predicts a solvation free energy of methanethiolate (−291.8 kJ mol^{-1}) much closer to the experimental value (−303.5 kJ mol^{-1}, ref 25) as compared to the IPCM method (−233.2 kJ mol^{-1}).

The same method recently applied to the study of the cysteine oxidation by the hydroxyl radical (OH$^{\bullet}$) gave an energy barrier higher by only 1.7 kJ mol^{-1} with respect to the experimental value.

Selenocysteine Residue Oxidation. The conformation of the selenocysteine residue as appearing in the X-ray diffraction structure of GPx[26] is very similar to that of the cys1 model in Figure 1. For the present calculation, the model system selcys1 was thus obtained by extracting the corresponding molecular fragment from the GPx experimental structure and by adding two methyl groups to the terminal N atoms. The model was then reoptimized both in vacuo and in aqueous solution. A second conformation, selcys2, was generated from the cys2 model by replacing the S atom by selenium. After reoptimization, the selcys2 conformation was very close to the starting configuration except, of course, for the Se−O distance.

The RC1 and TS1 configurations obtained in the same manner as for cysteine are represented in Figure 4. These structures are very similar to that obtained for cysteine. In particular, in the case of the TS1, one notes the H-bonding interaction between the NH group of selcys1 and the hydrogen peroxide.

When comparing the in vacuo TS1 structure with that reported for the CH_3Se^- model system,[9] one notes an increase of the Se−O distance by 0.02 Å and a decrease of the Se−H distance by about 0.05 Å. Obviously, these deviations are due to the inclusion of more atoms in the reactant system. As in the case of the cysteine residue, this inclusion induces also an increase of the effective reaction energy barrier which becomes 25.6 kJ mol^{-1} in vacuo (Table 2). This value is 7.4 kJ mol^{-1} greater than that reported for methanesolenolate.[9] The difference is still more important in aqueous solution, about 11.8 kJ mol^{-1}. Interestingly, the effective reaction energy barrier in aqueous solution, ΔG_{aq}(TS1), is only 1.8 kJ mol^{-1} lower than that calculated for the cysteine residue model cys1. It appears that the substitution of sulfur by selenium has little effect on the system reactivity. This is a confirmation of a previous result obtained by comparing the energy barriers for methanethiolate and methaneselenolate oxidation by H_2O_2.[9]

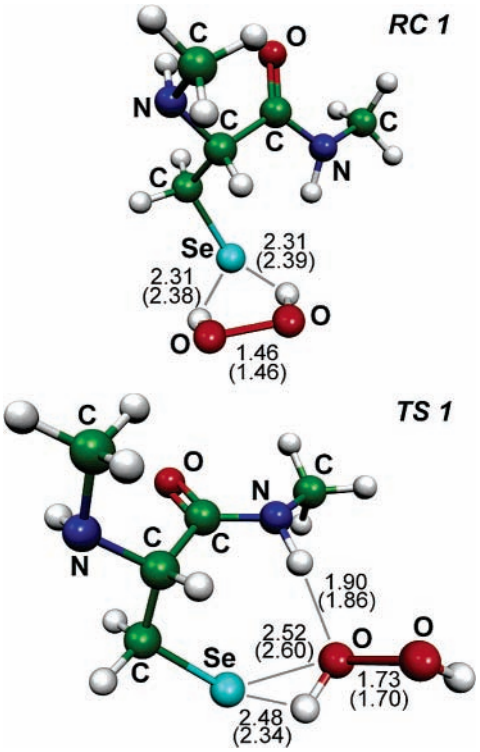

Figure 4. Oxidation of the selenocysteine residue model selcys1 by H_2O_2: the reactant complex RC1 and the transition-state TS1. Atomic distances are given in Å. Geometries were optimized in vacuo and in aqueous solution at the MP2/6-311+G(d,p) level of theory. The in vacuo atomic distances are given in parentheses.

The data in Table 2 also indicate that the energy barrier for the oxidation of the selcys2 residue model (Figure 5) in vacuo is higher by 8.7 kJ mol^{-1} with respect to that of the selcys1. However, in aqueous solution, the solvent interaction partially compensates this difference and the two energy barriers are separated by only 2.1 kJ mol^{-1}.

Now, we want to compare the reactivity of the free selenocysteine with that of GPx. No experimental energy barrier has been determined for the formation of the GPx-SeO$^-$ product (eq 1), but the experimental value of the corresponding reaction rate constant k_1 has already been reported.[7,8] It is also possible to calculate a theoretical value of k_1 for the selenocysteine residue in aqueous solution by using the energy barrier ΔG_{aq}(TS1a) in Table 2 and the Eyring equation

$$k^{TST} = (k_B T/h) c_0 \exp[-\Delta G_{aq}(TS)/RT] \qquad (8)$$

This equation gives the reaction rate constant in the conventional transition-state theory (TST). Here, k_B is the Boltzmann constant, h is the Planck constant, R is the gas constant, T is the temperature, and c_0 is the standard molar concentration in solution (1 mol dm^{-3}). For a ΔG_{aq}(TS1) value of 77.8 kJ mol^{-1}, eq 8 gives a k^{TST} of 0.18 mol^{-1} dm^3 s^{-1}. The theoretical rate constant calculated in the TST approximation may be further improved by performing a tunneling correction as indicated in ref 9. In the present case, a value of 1.36 was found for the

TABLE 2: Thermodynamic Parameters for the Selenocysteine Oxidation by H_2O_2[a]

	$E_{p,g}$ (Hartree)	$\Delta E_{0,g}$ (kJ mol^{-1})	ΔH_g (kJ mol^{-1})	ΔG_g (kJ mol^{-1})	G_{solv} (kJ mol^{-1})	ΔG_{aq}(kJ mol^{-1})
FR1	−2931.86841	0.0	0.0	0.0	−221.0	0.0
RC1	−2931.89906	−76.1	−76.1	−36.6	−178.0	6.4
TS1	−2931.87409	−17.2	−17.4	25.6	−168.8	77.8
FR2	−2931.84472	0.0	0.0	0.0	−260.3	0.0
RC2	−2931.87822	−83.6	−83.6	−41.7	−214.8	3.8
TS2	−2931.84798	−10.8	−11.0	34.3	−214.7	79.9

[a] The notations are similar to that described in the legend of Table 1.

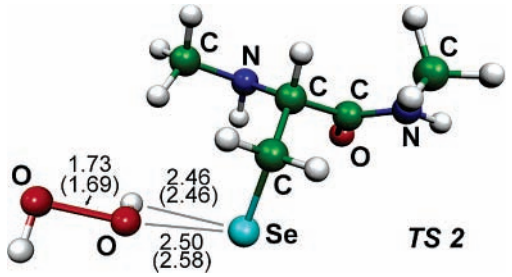

Figure 5. Oxidation of the selenocysteine residue model selcys2 by H_2O_2: the transition-state TS2. Atomic distances are given in Å. Geometries were optimized in vacuo and in aqueous solution at the MP2/6-311+G(d,p) level of theory. The in vacuo atomic distances are given in parentheses.

transmission coefficient to multiply k^{TST}. The corrected reaction rate constant is thus 0.25 mol^{-1} dm^3 s^{-1}. This value is far away from the experimental value of 5.0×10^7 mol^{-1} dm^3 s^{-1} reported for the GPx.[7,8] Obviously, there is no similarity whatsoever between the present deviation and the expected error in the theoretical energy barrier which is, according to the previous analysis, about 10 kJ mol^{-1}. On the other hand, the results in Table 2 show that the effective energy barrier for the selenocysteine residue oxidation is considerably lower in vacuo with respect to the aqueous solution. Hence, one could suppose that the actual difference between GPx and free selenocysteine is mainly due to the hydrophobic environment of the selenocysteine residue in GPx. However, the selenocysteine residue could not be completely buried in the protein structure as far as it is accessible for a rather large molecule such as GSH (in the second step of the GSH oxido-reduction cycle). A partial (at least) solvent accessibility is necessary to preserve a reasonable low pK_a value of selenocysteine. This partial accessibility is confirmed by the X-ray diffraction structure of the enzyme.[26] Moreover, it is known that at room temperature protein structure fluctuates significantly thus increasing the solvent accessibility of its residues.[27] One could roughly simulate the environment of the partially solvent-exposed residues by performing PCM calculations with a dielectric constant value intermediate between water and vacuum. It was already shown in the case of the methaneselenolate that this modification enhances significantly but not sufficiently the calculated reaction rate constant.[9] A more specific treatment of the selenocysteine residue environment should take into account the effect of the electric charges carried by the two lysine and four arginine residues around the selenocysteine. These positively charged residues have an important role in the stabilization of the GPx−glutathione complex in the second step of the H_2O_2 reduction cycle.[2] They could also play a role in stabilizing the deprotonated form of selenocysteine. In this context, a mixed quantum mechanics/molecular mechanics (QM/MM) study is expected to give a more realistic energy barrier. Such an approach will require, of course, a careful choice of the MM force field parameters to accurately describe the long-range electrostatic interactions here involved.

An alternative explanation for the low-energy barrier in the GPx oxidation is the possible H-bonding interaction between selenium atom and the imino group of the neighboring tryptophan residue or with the amido group of a glutamine residue which is situated at a favorable distance too.[28] This hypothesis is supported by the experimental result indicating that the absence of the tryptophan residue (as in the case of the selenoprotein P) is associated with an important decrease of the reaction rate constant k_1.[7] However, the mechanism of this energy-barrier lowering has not been demonstrated yet. Instead, our present results (compare ΔG_g(TS1a) and ΔG_g(TS1b) in Table 1) suggest that the H-bonding between the H_2O_2 and a NH group contribute to a nonnegligible decrease of the energy barrier, especially in a hydrophobic environment. This effect could be present in the case of GPx since the H_2O_2 can form H-bonds with the imino/amido group of tryptophan/glutamine residue.

Conclusions

The IMOMO method allowed us to calculate with satisfactory accuracy the energy barrier for cysteine and selenocysteine oxidation by H_2O_2 using realistic models for both amino acid residues. The analysis showed that the effects of the residue conformation on the reaction energy barrier and the reactants complexation energy are not negligible. On the other hand, the H-bonding between the peroxide and the NH group of amino acid residue was shown to significantly reduce the reaction energy barrier. These effects are strongly attenuated in aqueous solution.

It was also found that the free selenocysteine and cysteine have very similar reaction energy barriers. However, the calculated reaction rate constant for the free selenocysteine in aqueous solution is several orders of magnitude smaller than the experimental value reported for GPx. This result supports the idea that in the GPx case the reaction is strongly affected by the molecular environment of the selenocysteine residue. The main indications in this direction are the great sensitivity of the calculated energy barrier with respect to the PCM dielectric constant and the catalytic effect of the NH group observed in the case of cysteine.

Supporting Information Available: Cartesian coordinates for the transition-states TS1a, TS1b, and TS2 for cysteine oxidation and TS1 and TS2 for selenocysteine oxidation; Gaussian 03 ONIOM input job for single-point energy calculation on the transition-state TS1 of selenocysteine; Gaussian 03 PMP2+PCM input job for single-point energy calculation in aqueous solution on the same structure. This material is available free of charge via the Internet at http://pubs.acs.org.

References and Notes

(1) Lee, S. R.; Yang, K. S.; Kwon, J.; Lee, C.; Jeong, W.; Rhee, S. G. *J. Biol. Chem.* **2002**, *277*, 20336−20342.

(2) Ursini, F.; Maiorino M.; Brigelius-Flohé, R.; Aumann, K. D.; Roveri, A.; Schomburg, D.; Flohé, L. Diversity of glutathione peroxidases.

In *Biothiols Part B: Glutathione and Thioredoxin: Thiols in Signal Transduction and Gene Regulation;* Packer, L., Ed.; Methods in Enzymology; Academic Press: San Diego, CA, 1995; Vol. 252, pp 38−53.

(3) Lacourciere, G. M.; Stadtman, T. C. *Proc. Natl. Acad. Sci. U.S.A.* **1999**, *96*, 44−48.

(4) Kortemme, T.; Creighton, T. E. *J. Mol. Biol* **1995**, *253*, 799−812.

(5) Radi, R.; Beckman, J. S.; Bush, K. M.; Freeman, B. A. *J. Biol. Chem.* **1991**, *266*, 4244−4250.

(6) Winterbourn, C.; Metodiewa, D. *Free Radical Biol. Med.* **1999**, *27*, 322−328.

(7) Takebe, G.; Yarimizu, J.; Saito, Y.; Hayashi, T.; Nakamura, H.; Yodoi, J.; Nagasawa, S.; Takahashi, K. *J. Biol. Chem.* **2002**, *277*, 41254−41258.

(8) Maiorino, M.; Gregolin, C.; Ursini F. Phospholipid hydroperoxide glutathione peroxidase. In *Oxygen Radicals in Biological Systems Part B: Oxygen Radicals and Antioxidants;* Packer, L., Glazer, A. N., Eds.; Methods in Enzymology; Academic Press: New York, 1990; Vol. 186, pp 448−457.

(9) Cardey, B.; Enescu, M. *ChemPhysChem* **2005**, *6*, 1175−1180.

(10) Svensson, M.; Humbel, S.; Morokuma, K. *J. Chem. Phys.* **1996**, *105*, 3654−3661.

(11) Enescu, M.; Cardey, B. *ChemPhysChem* **2006**, *7*, 912−919.

(12) Pople, J. A.; Head-Gordon, M.; Raghavachari, K. *J. Chem. Phys.* **1987**, *87*, 5968−5975.

(13) Moller, C.; Plesset, M. S. *Phys. Rev.* **1934**, *46*, 618−622.

(14) Frisch, M. J.; Trucks, G. W.; Schlegel, H. B.; Scuseria, G. E.; Robb, M. A.; Cheeseman, J. R.; Montgomery, J. A., Jr.; Vreven, T.; Kudin, K. N.; Burant, J. C.; Millam, J. M.; Iyengar, S. S.; Tomasi, J.; Barone, V.; Mennucci, B.; Cossi, M.; Scalmani, G.; Rega, N.; Petersson, G. A.; Nakatsuji, H.; Hada, M.; Ehara, M.; Toyota, K.; Fukuda, R.; Hasegawa, J.; Ishida, M.; Nakajima, T.; Honda, Y.; Kitao, O.; Nakai, H.; Klene, M.; Li, X.; Knox, J. E.; Hratchian, H. P.; Cross, J. B.; Adamo, C.; Jaramillo, J.; Gomperts, R.; Stratmann, R. E.; Yazyev, O.; Austin, A. J.; Cammi, R.; Pomelli, C.; Ochterski, J. W.; Ayala, P. Y.; Morokuma, K.; Voth, G. A.; Salvador, P.; Dannenberg, J. J.; Zakrzewski, V. G.; Dapprich, S.; Daniels, A. D.; Strain, M. C.; Farkas, O.; Malick, D. K.; Rabuck, A. D.; Raghavachari, K.; Foresman, J. B.; Ortiz, J. V.; Cui, Q.; Baboul, A. G.; Clifford, S.; Cioslowski, J.; Stefanov, B. B.; Liu, G.; Liashenko, A.; Piskorz, P.; Komaromi, I.; Martin, R. L.; Fox, D. J.; Keith, T.; Al-Laham, M. A.; Peng, C. Y.; Nanayakkara, A.; Challacombe, M.; Gill, P. M. W.; Johnson, B.; Chen, W.; Wong, M. W.; Gonzalez, C.; Pople, J. A. *Gaussian 03*, Revision B.04; Gaussian, Inc.: Pittsburgh, PA, 2003.

(15) Cossi, M.; Scalmani, G.; Rega, N.; Barone, V. *J. Chem. Phys.* **2002**, *117*, 43−54.

(16) Chen, W.; Schlegel, H. B. *J. Chem. Phys.* **1994**, *101*, 5957−5968.

(17) Luo, D.; Smith, S. W.; Anderson, B. D. *J. Pharm. Sci.* **2005**, *94*, 304−316.

(18) Gonzalez, C.; Schlegel, H. B. *J. Phys. Chem.* **1990**, *94*, 5523−5527.

(19) Chu, J. W.; Trout, B. L. *J. Am. Chem. Soc.* **2004**, *126*, 900−908.

(20) Schwenke, D. W.; Truhlar, D. G. *J. Chem. Phys.* **1985**, *82*, 2418−2426.

(21) Dunning, T. H., Jr. *J. Phys. Chem. A* **2000**, *104*, 9062−9080.

(22) Boys, S. F.; Bernardi, F. *Mol. Phys.* **1970**, *19*, 553−557.

(23) Ayala, P. Y.; Schlegel, H. B. *J. Chem. Phys.* **1997**, *108*, 2314−2325.

(24) Foresman, J. B.; Keith, T. A.; Wilberg, K. B.; Snoonian, J.; Frisch, M. J. *J. Phys. Chem.* **1996**, *100*, 16098−16104.

(25) Pliego, J. R., Jr.; Riveros, J. M. *J. Phys. Chem. A* **2001**, *105*, 7241−7247.

(26) Epp, O.; Ladenstein, R.; Wendel, A. *Eur. J. Biochem.* **1983**, *133*, 51−69.

(27) Chu, J. W.; Yin, J.; Wang, D. I. C.; Trout, B. L. *Biochemistry* **2004**, *43*, 1019−1029.

(28) Mugesh, G.; du Mont, W. W. *Chem. Eur. J.* **2001**, *7*, 1365−1370.